some extent destroy the structural symmetry of the test piece, which in turn increases the measured cross-polarized radiation, especially in the E-plane. The measured cross-polarized pattern in Fig. 10 is even pronounced due to the unwanted scattered fields from the surrounding measurement facilities. This also causes some measurement uncertainties in the measured co-polarized components in both principle planes. Nonetheless, the cross-polarization level measured in both principle planes still remains satisfactorily low. The simulated and measured peak gains are 3.8 dBi and 3.6 dBi, respectively, while the simulated and measured radiation efficiencies are 84% and 80%. Compared to that of the conventional designs operating at first harmonic mode [5]–[9], the peak gain of the prototype antenna is slightly lower and remains satisfactory since the antenna area is greatly reduced (about 88.9% reduction in size).

V. Conclusion

In this communication, the fundamental and harmonic resonances of the slot loop antenna inductively fed by a CPW are investigated. Note that, traditionally, the inductively fed slot loop antennas can be designed only at the second or higher-order harmonic modes. By placing a pair of folded thin strips across the coupled slotlines of the feeding CPW and narrowing the protruded section of the signal trace of the CPW, the impedance matching of the antenna at the fundamental mode can be achieved, and the higher-order resonant modes can be suppressed at the same time. The prototype antenna is demonstrated to be able to operate at the fundamental resonant frequency of 2.5 GHz. It radiates as a slot antenna in a finite ground plane and shows a wideband harmonic suppression of at least up to 20 GHz. Besides, the antenna area is only 1/9 of the conventional design that is operated at its second harmonic mode and only 1/4 of the capacitively fed slot loop antenna operating at its fundamental resonance. Although the impedance bandwidth of the prototype antenna with a square shaped slot loop is narrow, it can be improved simply by increasing the aspect ratio of the slot loop, making our proposed design feasible for narrowband mobile communications, such as WiFi, Bluetooth, GPS, etc.

References

[1] D. Llorens, P. Otero, and C. Camacho-Penalosa, "Dual-band, single CPW port, planar-slot antenna," *IEEE Trans. Antenna Propag.*, vol. 51, no. 1, pp. 137–139, Jan. 2003.

[2] W.-S. Chen and K.-L. Wong, "A coplanar waveguide-fed printed slot antenna for dual-frequency operation," in *Proc. IEEE AP-S Int. Symp.*, Boston, MA, USA, Jul. 2001, pp. 140–143.

[3] J.-S. Chen, "Studies of CPW-fed equilateral triangular-ring slot antennas and triangular-ring slot coupled patch antennas," *IEEE Trans. Antennas Propag.*, vol. 53, no. 7, pp. 2208–2211, Jul. 2005.

[4] S. V. Shynu and M. J. Ammann, "A printed CPW-fed slot loop antenna with narrowband omnidirectional features," *IET Microwaves, Antennas Propag.*, vol. 3, no. 4, pp. 673–680, Jun. 2009.

[5] S.-W. Lu, C.-H. Yang, and P. Hsu, "A CPW-fed slot-loop antenna with low cross-polarization radiation," in *Proc. Asia-Pacific Microw. Conf.*, Sydney, Australia, Dec. 2000, pp. 1400–1402.

[6] M.-H. Yeh, P. Hsu, and J.-F. Kiang, "Analysis of a CPW-fed slot ring antenna," in *Proc. Asia-Pacific Microw. Conf.*, Taipei, Taiwan, Dec. 2001, pp. 1267–1270.

[7] Y.-C. Chen, S.-Y. Chen, and P. Hsu, "A modified CPW-fed slot loop antenna with reduced cross-polarization and size," *IEEE Antennas Wireless Propag. Lett.*, vol. 10, pp. 1124–1126, 2011.

[8] X.-C. Lin and L.-T. Wang, "A broadband CPW-fed loop slot antenna with harmonic control," *IEEE Antennas Wireless Propag. Lett.*, vol. 2, pp. 323–325, 2003.

[9] H.-D. Chen, "Broadband CPW-fed square slot antenna with a widened tuning stub," *IEEE Trans. Antenna Propag.*, vol. 51, no. 8, pp. 1982–1986, Aug. 2003.

[10] K.-C. Chi, S.-Y. Chen, and P. Hsu, "Miniaturization of slot loop antenna using split-ring resonator," presented at the IEEE AP-S Int. Symp., Charleston, SC, USA, Jun. 2009.

[11] P.-L. Chi, K. M. Leong, R. Waterhouse, and T. Itoh, "A miniaturized CPW-fed capacitor loaded slot-loop antenna," in *Int. Symp. Signals, Systems and Electronics*, 2007, pp. 595–598.

[12] P.-L. Chi, R. Waterhouse, and T. Itoh, "Antenna miniaturization using slow wave enhancement factor from loaded transmission line models," *IEEE Trans. Antenna Propag.*, vol. 59, no. 1, pp. 48–57, Jan. 2011.

[13] M. S. Ghaffarian and G. Moradi, "A novel harmonic suppressed coplanar waveguide (CPW)-fed slot antenna," *IEEE Antennas Wireless Propag. Lett.*, vol. 10, pp. 788–791, 2011.

[14] D. M. Pozar, *Microwave Engineering*, 2nd ed. New York, NY, USA: Wiley, 1998.

A Dual-Resonant Shorted Patch Antenna for Wearable Application in 430 MHz Band

Han Wang, Zhijun Zhang, Yue Li, and Zhenghe Feng

***Abstract*—In this communication, a novel approach to expand the bandwidth for the ultra-low profile wearable shorted patch is proposed and fabricated. It introduces dual-resonance to acquire 5.2% bandwidth within $0.358\lambda \times 0.358\lambda \times 0.011\lambda$ dimension at 430 MHz without increasing the structure complexity. By using EVA (ethylene-vinyl acetate) foam and copper gauze as the material, this dual-resonant shorted patch is light, flexible, and rigid enough for wearable application. SAR (special absorption rate) and performance after bending are simulated and analyzed to validate its reliability in wearable condition. The measurement result verifies the design concept, which can provide consistent radiation character, along with acceptable gain and efficiency in the whole working band.**

***Index Terms*—Bandwidth expansion, impedance matching, patch antenna, wearable antenna.**

I. Introduction

Due to its superb propagation characteristics, the UHF band is widely used in long rang communication devices, such as law enforcement radios, Walkie Talkie and ISM (Industrial Scientific and Medical) devices, etc. In some special scenarios, the radio is required to be concealed under cloth and still maintain its capability of handling frequency duplex. To meet these requirements, the antenna design should be wearable, light weight, least affected by human body, and most importantly, very low-profile (below 10 mm) with sufficient bandwidth.

Among many candidates, shorted patch or planar invert-F antenna (PIFA) is one of the most promising designs owing to its simple structure and unidirectional radiation character. With the ground shielding, it is less affected by human body, and can offer sufficient bandwidth

Manuscript received August 30, 2012; revised April 03, 2013; accepted July 01, 2013. Date of publication September 16, 2013; date of current version November 25, 2013. This work was supported in part by the National Basic Research Program of China under Contract 2009CB320205, in part by the National High Technology Research and Development Program of China (863 Program) under Contract 2011AA010202, the National Natural Science Foundation of China under Contract 61271135, the China Postdoctoral Science Foundation funded project 2013M530046, and the National Science and Technology Major Project of the Ministry of Science and Technology of China 2013ZX03003008-002 and Qualcomm Inc.

The authors are with the State Key Lab. of Microwave and Communications, Tsinghua National Laboratory for Information Science and Technology, Tsinghua University, Beijing 100084, China (e-mail: zjzh@tsinghua.edu.cn).

Color versions of one or more of the figures in this communication are available online at http://ieeexplore.ieee.org.

Digital Object Identifier 10.1109/TAP.2013.2282044

for 900 MHz and 2.4 GHz design [1]–[3] at adequate height (0.05λ or more). However, when the working frequency reduces to 430 MHz, the wavelength reaches around 0.7 meter, and the substrate would be too thick to conceal if applying traditional design (around 35 mm at 0.05λ). If further reduces the height into 10 mm (0.014λ), the bandwidth would be too narrow (around 2%) to support the frequency duplex. Thus, it is very challenging to design an ultra low-profile patch with sufficient bandwidth at this frequency.

In existent researching literatures, S. Villers [4] has proposed a patch design with 7.3 mm thickness at 400 MHz. However, the bandwidth is only 3 MHz. Sarabandi *et al.* [5] has used U-slot with ceramic load to acquire 20% bandwidth in 450 MHz, Nonetheless, its height is around 0.05λ (30 mm) and the substrate is hard and rigid. Some reports have focused on feeding techniques, including staked feed [6] and L-probe feed [7]. Nevertheless, their heights are still too high, and it is difficult to implement them in massive production due their structure complexity. Withal, Aperture couple is a prominent broadbanding technique proposed in [8]. However, with a back lobe radiation, its performance is easily affected by the presence of human body. Furthermore, Xiao *et al.* [9] presents a wideband ultra-low-profile patch, which tunes multi-mode together to broaden the bandwidth. However, it is based on $\lambda/2$ structure and uses high dielectric substrate to lower the height and drive multi-modes together. Thus, its size would be large and the substrate would be bulky if applying in 430 MHz.

In this communication, we propose an patch design and corresponding matching method to attain around 5.2% bandwidth at 430 MHz with a 150 mm × 137 mm ($0.215\lambda \times 0.197\lambda$) patch placed on a 250 mm × 250 mm × 8 mm ($0.358\lambda \times 0.358\lambda \times 0.011\lambda$) substrate. Dual-resonant character has been achieved and the bandwidth has been doubled comparing with the conventional design at the same height. In addition, to properly meet the wearable requirement, EVA (ethylene-vinyl acetate) foam and copper gauze are selected as substrate and conductor in this communication. It is flexible, deformation resistant, sewable, and can be easily applied in large-scale production with traditional processing technique.

In the following contents, Section II introduces the antenna design and matching technique to realize dual-resonant character; Section III provides some details about the material and presents a prototype built with the proposed technique; Section IV presents the simulation/measuring result acquired with the proposed design. Performance after bending is analyzed and SAR (Special Absorption Rate) is simulated under IEEE 1528 standards [10]. Test results are measured in a commercial chamber, which include some results tested with/without human body.

II. Antenna Design and Matching

Fig. 1(a) shows a traditional shorted patch design. By implementing a shorting wall along one edge, it is half the size of a $\lambda/2$ patch and the matching can be realized by tuning the feeding position d_{offset} along the symmetric axis. Fig. 1(b) presents the proposed design. The feeding position is moved into a central cut at the shorting edge, and the width of the central cut $d_{\rm cut}$ is facilitated as the tuning parameter.

Fig. 2(a) shows the impedance loci of these two designs. The dash line without marker is the impedance locus of the traditional design when $d_{offset} = 32$ mm. The solid lines with different markers are impedance loci of the proposed antenna when $d_{\rm cut}$ takes different values. It can be noticed that both designs have a similar single resonant character when $d_{\rm cut} = 64$ mm, and an equivalent circuit, which reflects such impedance character, is proposed and given in this figure.

In this circuit, the series inductor L_f has more impact on the higher band, thus the loci's higher end would shift up into the upper left area of the Smith Chart as shown in Fig. 2(a). A loop would be formed

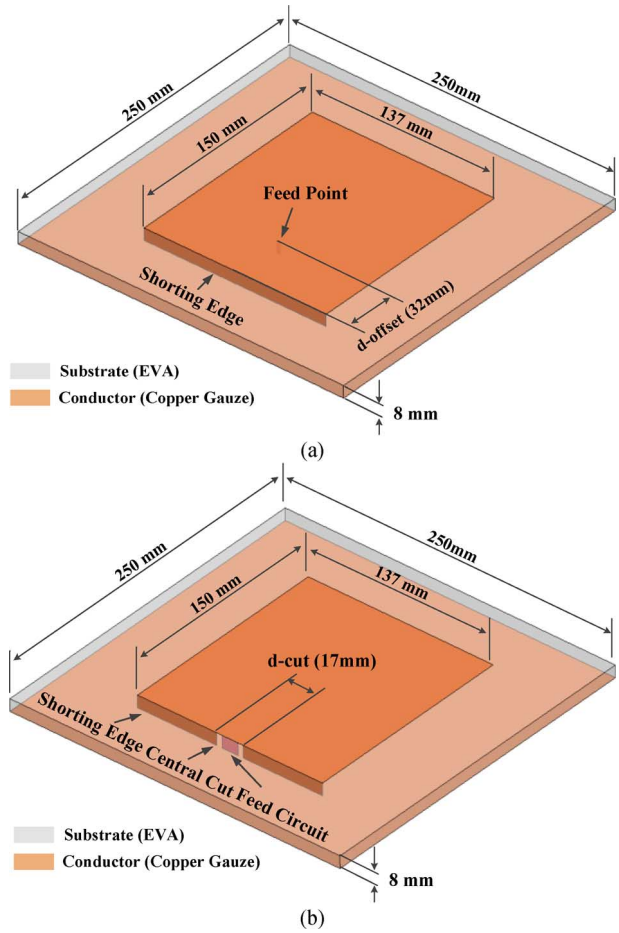

Fig. 1. (a) Geometry of the traditional shorted patch. (b) Geometry of the proposed shorted patch.

when the loci's higher band intersects with the lower band, and it would shrink toward the upper left corner on the Smith Chart by decreasing d_{cut}. Similar phenomenon can be observed by decreasing L_p. Thus, in this proposed design, the equivalent inductor L_p can be adjusted and utilized directly.

To expand the bandwidth, two additional components C_m and L_m are introduced to realize dual-resonance. With the adjustable equivalent inductor L_p, a π-shape network (L_p, C_m and L_m) is formed as shown in Fig. 3. It is an effective circuit topology to widen the bandwidth [11], and the principle of the matching method can be briefly introduced as follows:

1) Adjust the d_{cut} value to tuning the L_p, attain a suitable impedance loop size as shown in Fig. 2(a).
2) Add a series capacitor C_m to the antenna. Adjust its value to move the impedance loop to the admittance circle ($Y = 1$) at the lower left side of the Smith Chart as shown in Fig. 2(b).
3) Add a shunt inductor L_m to the port. Adjust its value to further pull the loop up into the desired matching circle ($\Gamma < -10$ dB in this case) as shown in Fig. 2(b).

Once these three steps are performed, the original impedance locus becomes that shown in Fig. 2(b). The intersection point can be clearly observed in the matching circle, which will present a dual-resonant character as shown in Fig. 5. Comparing with the single resonant impedance character shown in Fig. 2(a), The bandwidth reaches around 5.2% (22.3 MHz from 417.8 MHz to 440.1 MHz as the grey area indicating) in this case, which is doubled comparing to 2.4% (10 MHz) in traditional design.

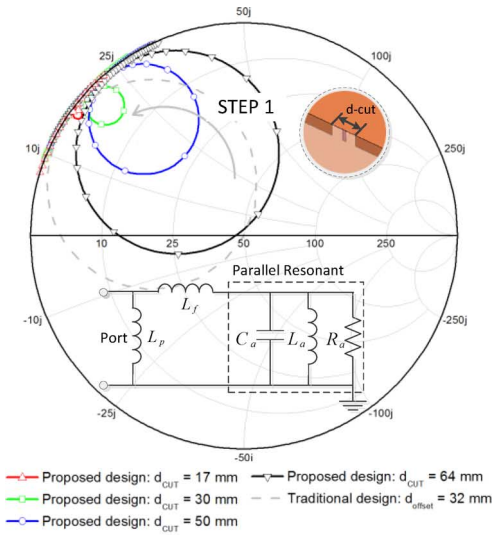

(a)

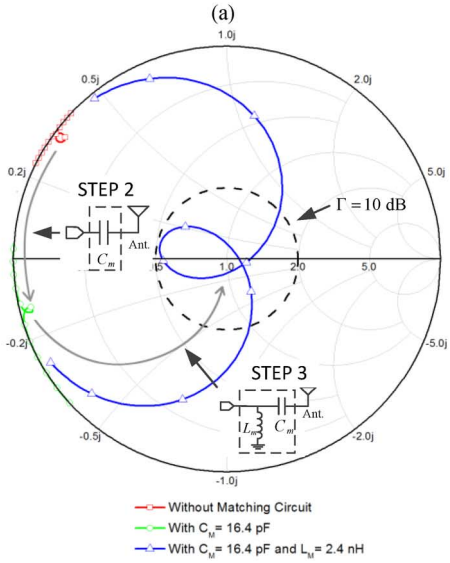

(b)

Fig. 2. The impedance loci of the shorted patch and the proposed matching method. (a) The effect of tuning d_{cut} and the equivalent circuit of the proposed patch. (b) The effect of adding matching component C_m and L_m.

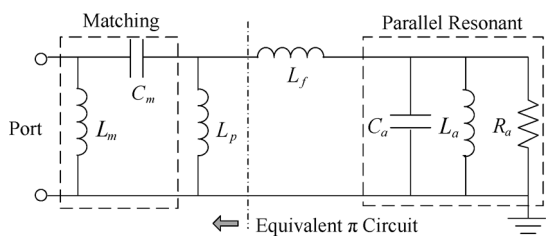

Fig. 3. The matching method and the equivalent π-shape matching network.

For validation purpose, Fig. 4 provides the input impedance comparison between the full wave simulation (HFSS) and the equivalent circuit based simulation (MWO). It can be noticed that all these traces match well and corresponding components' value are listed in this figure.

Since the shunt inductance L_p is generated by the structure itself and can be adjusted by tuning $d_{\rm cut}$, only two lump elements are needed to realize the matching. In the following section, to further reduce the manufacture complexity, this number will be further reduced to one by realizing the C_m with a distributed feature.

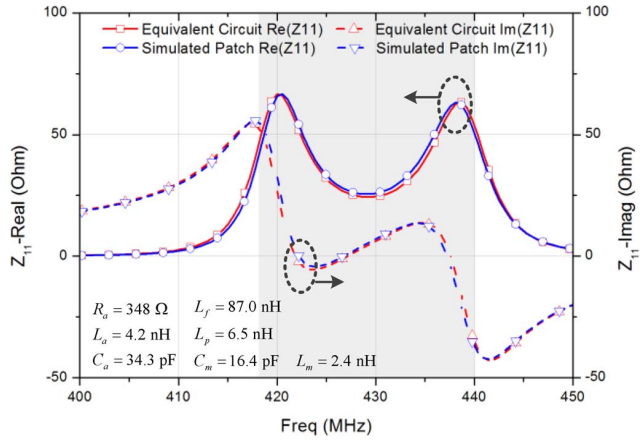

Fig. 4. The input impedance comparison between the full-wave simulation and the equivalent circuit based simulation after matching.

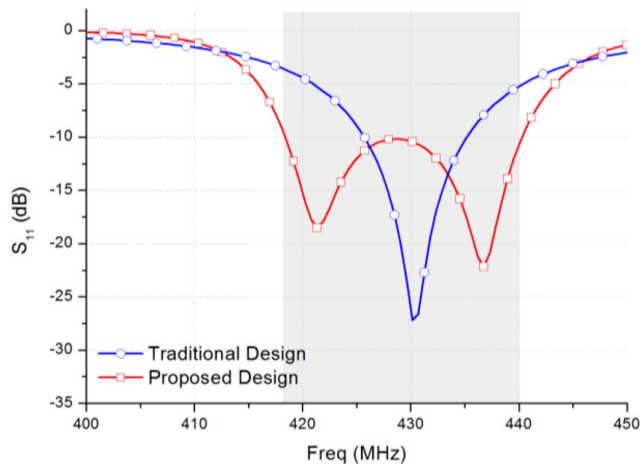

Fig. 5. The simulated S-parameter comparison between the proposed design and the traditional design after matching.

III. Material and the Prototype Build

By reviewing recently proposed wearable antennas designs [12]–[15], it can be noticed that most of them are based on flexible textile such as conductive thread based fabric and copper foil tap. They are light, flexible and sewable as traditional fabric, which can be integrated into cloth easily.

However, owing to the comparatively large size for the 430 MHz design, these flexible materials cannot provide enough rigidity to encounter the bending and crumpling brought about by body movement. The resonance will be affected and the radiation character will change, which may result in performance deterioration [16]. Consequently, the material should be not only flexible but also rigid enough to encounter deformation for this 430 MHz design.

Motived by this requirement, EVA material with very high foaming rate is chosen as the substrate. It is light, flexible but with adequate rigidity. This material, shown in Fig. 6(a), could be easily acquired at very low price ($ 1.25/m^2 in retail market). Owing to the high foaming rate, the density is very low and the electric character is similar to that

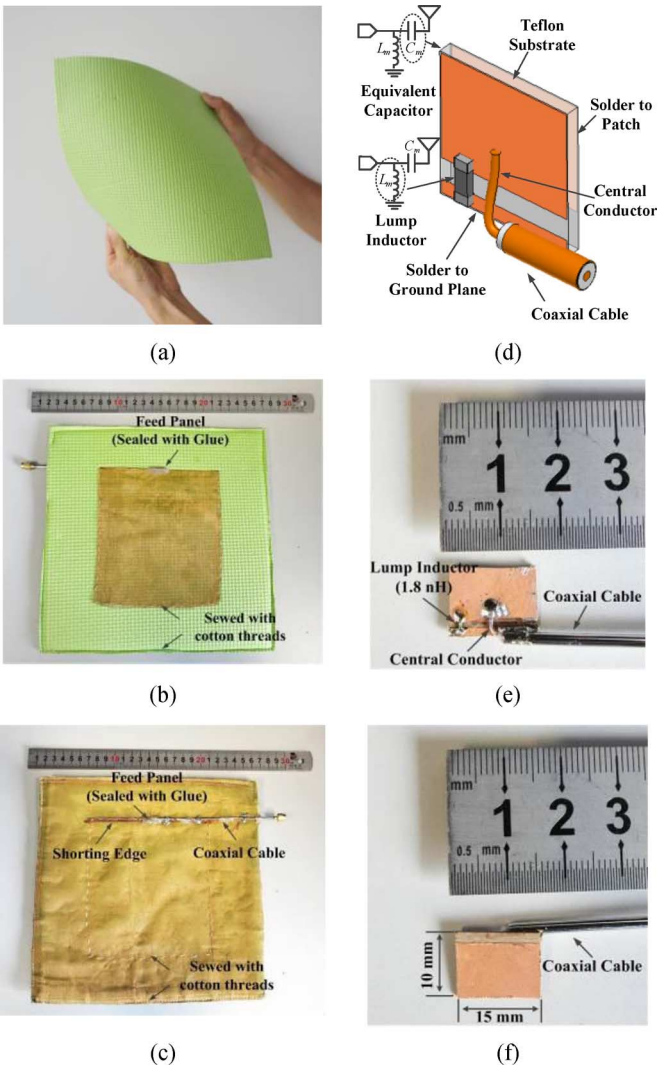

Fig. 6. (a) The EVA material. (b) The front side of the prototype. (c) The back side of the prototype. (d) The structure diagram of the feed panel. (e) The front side of the feeding panel. (f) The back side of the feeding panel.

of air with very low $\varepsilon_r \approx 1.10 - 1.20$ (1.17 in this design) and loss $\tan\delta \approx 0.004$, which is applicable for 430 MHz design.

The conductor selection is also based on the flexible and sewable requirement. Metal fiber implanted textiles is one promising candidate [17]. However, it is not suitable for implementation with a feed network due to its lack of soldering ability. Consequently, copper gauze with 150 meshes/inch ^{2} is selected for this design, which has the same soldering ability as copper wire and has good flexibility to be sewn on the EVA substrate with regular cotton thread. Furthermore, the cross-weaving copper wire with high mesh density of this material can guarantee high conductivity and low metallic loss, which is very similar to copper plate at 430 MHz.

The prototype is built with the geometry shown in Fig. 1(b). A photo of this prototype is presented in Fig. 6(b),(c), where white color cotton threads are used to stitch the structure together. To maintain the patch's advantages of simple structure and high radiation efficiency, a feed panel, built with a thin double-sided ceramic-PTFE board, is introduced in this design to realize matching and feeding. As shown in Fig. 6(d), this feed panel is inserted into the substrate vertically at the cutting slot and soldered with the upper patch and lower ground at opposite sides. A closer view is shown in Fig. 6(e),(f), where only one lumped

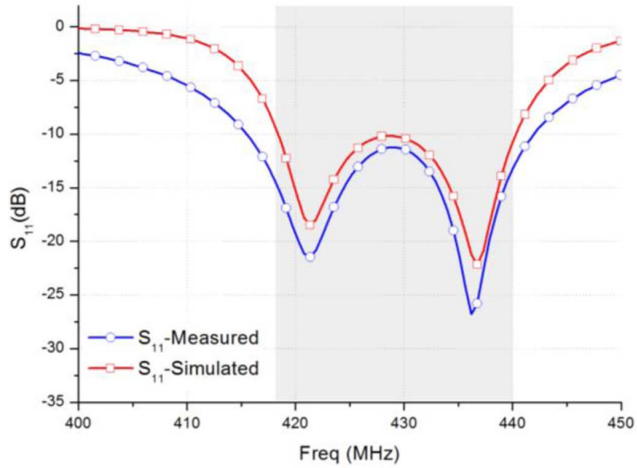

Fig. 7. The simulated and measured S-parameter of the proposed antenna.

inductor L_m is used since this board can provide distributed capacitor C_m between two layers. The board is 10 mm × 15 mm × 0.8 mm (2 mm height redundancy is reserved for soldering and tuning) in dimension with $\varepsilon_r = 9.7$ and $\tan\delta = 0.002$, which could provide a low loss 16.1 pF capacitor to realize the matching as describe in the previous section.

Benefit from this feed panel design, the C_m value is easy to tune by trimming the panel's redundant height, and the panel can be sealed with glue after soldering, which is easy to implement and can guarantee its reliability in mass production. Following the three matching steps described in the previous section, a 1.8 nH lump inductor is chosen, and the measured result is provided in Section IV.

IV. Simulation and Measurement Result

A. S-Parameter

The S-parameter was simulated in HFSS and the measurement was conducted with Agilent Vector Network Analyzer E5071B. As presented in Fig. 7, the measured result, with two resonant peaks at 421 MHz and 437 MHz, matches well with the simulated one, and the prototype attained around 28 MHz (6.5%) bandwidth in the measurement, which may be caused by additional loss in substrate, feed network and cable.

B. Radiation Pattern

The pattern was measured in an ETS-LINDGRENT AM8600 Chamber. Fig. 8 gives the 3D measurement results along with the radiation pattern for X-O-Y and X-O-Z plane from 420 to 440 MHz, which yields a similar result as the one acquired in full-wave simulation. It can be observed that the pattern maintains good consistency in full bandwidth, and the "doughnut"-shaped pattern in cross-polarization is mainly generated by the strong X-direction current at feed position.

The current distribution is also presented in Fig. 8, which verifies that this dual-resonant shorted patch works in identical TM_{10} mode as the traditional patch. The proposed bandwidth expansion technique does not affect its radiation character.

C. Gain and Efficiency

The measured gain and efficiency is provided in Fig. 9 with a comparison to the simulated one. Owing to the additional loss that may be introduced by the feed network and cable, the peak gain is 4.36 dB at 430 MHz, which is 0.50 dB lower than the simulated 4.86 dB in 433 MHz, and a degradation in gain and efficiency could be observed when

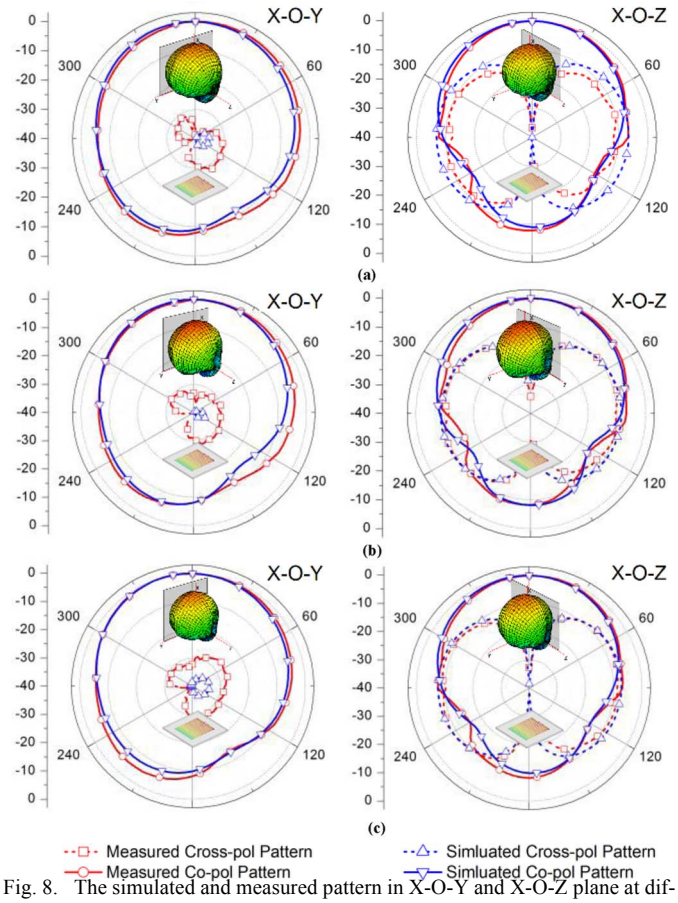

Fig. 8. The simulated and measured pattern in X-O-Y and X-O-Z plane at different frequency.

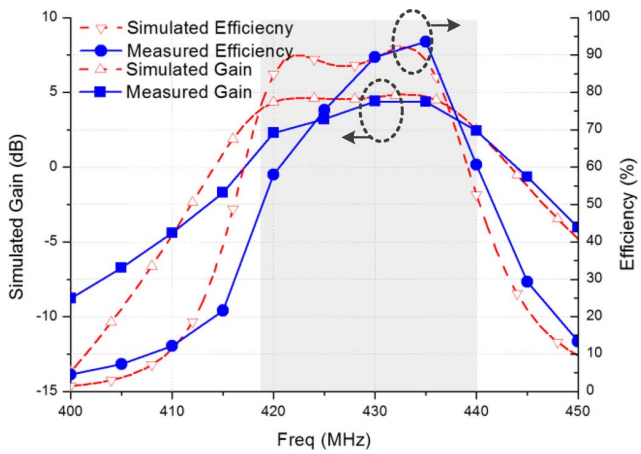

Fig. 9. The simulated and measured Gain/Efficiency.

deviated from the center frequency. However, this proposed dual-resonant shorted patch still achieve more than 2.41 dB gains and 51% efficiency in the whole working bands, which is acceptable in the trade of double bandwidth when compares with the traditional design.

D. Special Absorption Rate (SAR)

For wearable antenna design, the specific absorption rate (SAR) is an important measure criterion for safety consideration. Lower SAR indicates that less radiation is absorbed by the body.

For the proposed patch antenna, the SAR is simulated with 1 Watt transmitting power averaging in 1 g tissue. The entire simulation environment, including dielectric constant of the tissue, the size of the

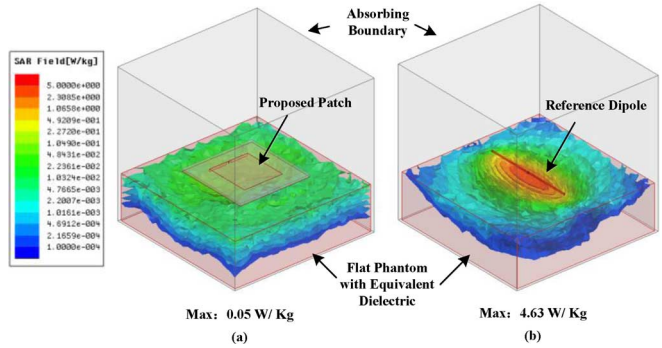

Fig. 10. The simulated SAR (special absorbing rate) comparison between (a) the proposed antenna and (b) the reference dipole.

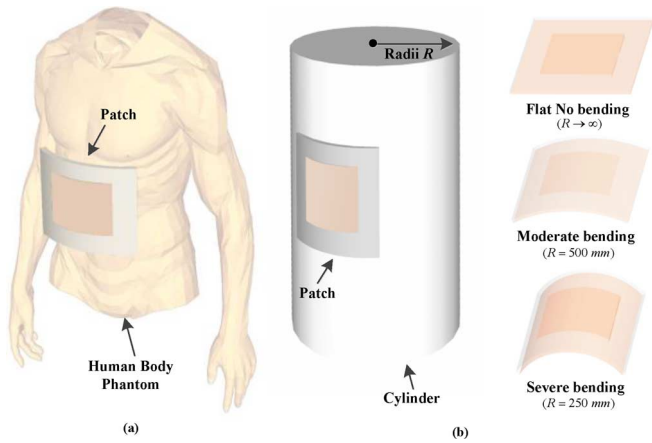

Fig. 11. (a) Typical application scenery when wearing. (b) The model and different bending conditions used in simulation.

flat phantom and the simulation scenery are set under IEEE 1528 standard [10]. The simulation result is provided in Fig. 10, where a dipole is shown as a reference. The proposed antenna's SAR (0.05 W/kg at 430 MHz) is much lower than the reference dipole (4.63 W/Kg at 430 MHz) and the FCC limitation (1.60 W/kg). This can be explained by the patch's unidirectional radiation character.

E. Bending and Its Effect on Antenna Performance

Due to its flexibility, wearable antenna is subjected to bending and crumpling when wearing. It may cause frequency shift and performance deterioration [16]. Comparing with the pure textile antenna proposed in [12]–[15], the EVA based antenna is rigid enough to resist against crumpling. However, bending along body surface is still unavoidable. To validate its performance and stability in all condition, a study on bending effect is performed in this section. The different bending curvatures are simulated by attaching the proposed antenna onto a cylinder with different radii R (Fig. 11(b)). Three different conditions, which includes flat no bending ($R \rightarrow \infty$), moderate bending ($R = 500$ mm) and severe bending ($R = 125$ mm), are analyzed as shown in Fig. 11(b). Owing to its low operating frequency, the proposed antenna is prefer to be mounted on the front chest or body back as shown in Fig. 11(a), Thus, moderate bending is more likely to happen since the curvature is much more moderate comparing with the one bending on arm or leg. Fig. 12 shows the performance change while bending. It can be noticed that even with severe bending that merely happens, the resonant frequency only shifts around 5 MHz and a 22 MHz bandwidth can still be acquired under -6 dB criteria.

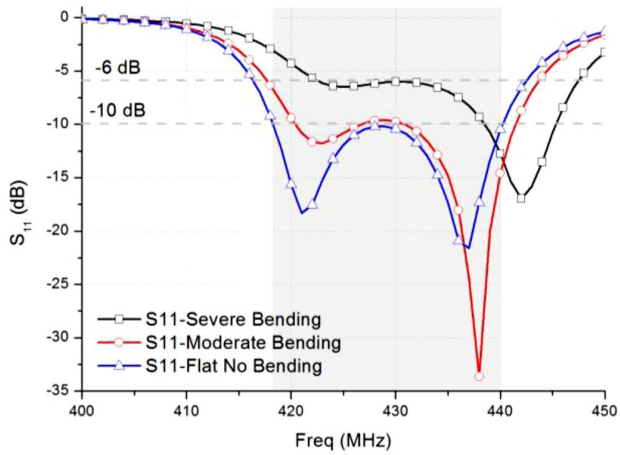

Fig. 12. The S-parameter of the proposed antenna at different bending conditions.

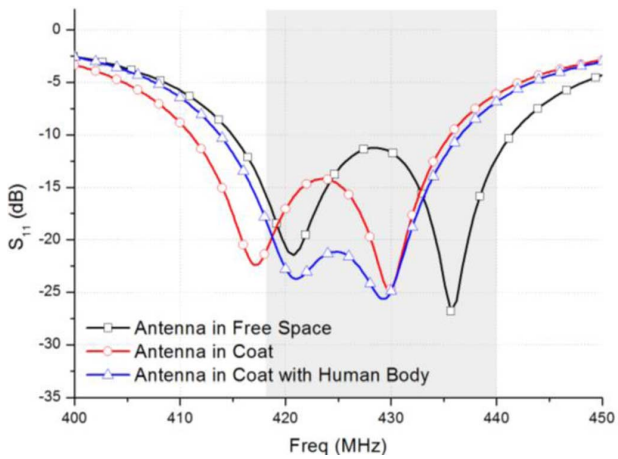

Fig. 13. S-parameter for the implanted dual-resonant shorted patch with/without human body.

(a) (b)

Fig. 14. (a) Antenna implant in cloth, and (b) the 2D measurement in Chamber with human body.

F. Test on Body

To verify its performance in wearing condition, the proposed shorted patch was implanted in a cotton coat as shown in Fig. 14(a). Measurement is taken with/without human body, and the S-parameter measurement is shown in Fig. 13. The resonant peak shifts at around 5 MHz towards lower frequency with the load from the coat. Owing to the unidirectional radiation character, the resonant form is not very sensitive to body load. The variation is not large and the peak is deeper when wear on high-loss human body, which proves that it is suitable for wearing application.

Finally, a 2D measurement was carried out for both wearing and take-off conditions as shown in Fig. 14(b). Around 1.5 dB gain loss is observed in the test, which is acceptable in wearable application.

V. Conclusion

In this communication, an ultra-low profile $(0.358\lambda \times 0.358\lambda \times 0.011\lambda)$ wearable patch working at 430 MHz is proposed and built. By using the EVA foam and the copper gauze as material, it is light, flexible and can be process with traditional manufacturing techniques. To expand the bandwidth, a three-step matching method is proposed to realize a dual-resonant character, which doubles the bandwidth (5.2%) comparing with the traditional design. The simulation and test result verifies that it has a consistent radiation character, along with acceptable gain and efficiency in full working bands. Furthermore, the SAR is very low and the performance is not sensitive to body load, cloth load or deformation, which is very suitable for wearable application.

References

[1] A. Tronquo, H. Rogier, C. Hertleer, and L. Van Langenhove, "Robust planar textile antenna for wireless body LANs operating in 2.45 GHz ISM band," *Electron. Lett.*, vol. 42, no. 3, pp. 142–143, Feb. 2006.

[2] S. Zhu and R. Langley, "Dual-band wearable textile antenna on an EBG substrate," *IEEE Trans. Antennas Propag.*, vol. 57, no. 4, pp. 926–935, Apr. 2009.

[3] X. Gao, Z. Zhang, W. Chen, Z. Feng, M. F. Iskander, and A.-P. Zhao, "A novel wrist wear dual-band diversity antenna," in *Proc. IEEE Int. Symp. Antennas and Propag. Society*, Jun. 2009, pp. 1–4.

[4] S. Villers, "Patch antenna with reduced size for 400 MHz transmission in confined surroundings," in *Proc. EuCAP. 1st Eur. Conf. on Antennas and Propagation*, Nov. 2006, pp. 1–4.

[5] K. Sarabandi, A. M. Buerkle, and H. Mosallaei, "Compact wideband UHF patch antenna on a reactive impedance substrate," *IEEE Antennas Wireless Propag. Lett.*, vol. 5, no. 1, pp. 503–506, Dec. 2006.

[6] J. Ollikainen, M. Fischer, and P. Vainikainen, "Thin dual-resonant stacked shorted patch antenna for mobile communications," *Electron. Lett.*, vol. 35, no. 6, pp. 437–438, Mar. 1999.

[7] C. L. Mak, K. M. Luk, K. F. Lee, and Y. L. Chow, "Experimental study of a microstrip patch antenna with an L-shaped probe," *IEEE Trans. Antennas Propag.*, vol. 48, no. 5, pp. 777–783, May 2000.

[8] C. Hertleer, A. Tronquo, H. Rogier, L. Vallozzi, and L. Van Langenhove, "Aperture-coupled patch antenna for integration into wearable textile systems," *IEEE Antennas Wireless Propag. Lett.*, vol. 6, pp. 392–395, 2007.

[9] S. Xiao, B.-Z. Wang, W. Shao, and Y. Zhang, "Bandwidth-enhancing ultralow-profile compact patch antenna," *IEEE Trans. Antennas Propag.*, vol. 53, no. 11, pp. 3443–3447, Nov. 2005.

[10] *IEEE Recommended Practice for Determining the Peak Spatial-Average Specific Absorption Rate (SAR) in the Human Head From Wireless Communications Devices: Measurement Techniques Amendment 1: CAD File for Human Head Model (SAM Phantom)*, IEEE Std. 1528a-2005 (Amendment to IEEE Std. 1528-2003), 2006.

[11] Z. Zhang, *Antenna Design for Mobile Devices*. Hoboken, NJ, USA: Wiley, 2011, pp. 35–48.

[12] O. Yuehui and W. J. Chappell, "High frequency properties of electro-textiles for wearable antenna applications," *IEEE Trans. Antennas Propag.*, vol. 56, no. 2, pp. 381–389, Feb. 2008.

[13] S.-J. Ha and C.-W. Jung, "Reconfigurable beam steering using a microstrip patch antenna with a U-slot for wearable fabric applications," *IEEE Antennas Wireless Propag. Lett.*, vol. 10, pp. 1228–1231, 2011.

[14] J. G. Santas, A. Alomainy, and Y. Hao, "Textile antennas for on-body communications: Techniques and properties," presented at the 2nd Eur. Conf. on Antennas and Propagation, Nov. 2007.

[15] F. Declercq and H. Rogier, "Active integrated wearable textile antenna with optimized noise characteristics," *IEEE Trans. Antennas Propag.*, vol. 58, no. 9, pp. 3050–3054, Sep. 2010.

[16] Q. Bai and R. Langley, "Crumpling of PIFA textile antenna," *IEEE Trans. Antennas Propag.*, vol. 60, no. 1, pp. 63–70, Jan. 2012.

[17] N. H. M. Rais, P. J. Soh, F. Malek, S. Ahmad, N. B. M. Hashim, and P. S. Hall, "A review of wearable antenna," in *Proc. Antennas Propagation Conf.*, Nov. 2009, pp. 225–228.